Flame Propagation Speed of CO2 Diluted Hydrogen-Enriched Natural Gas and Air Mixtures

ARTICLE *in* ENERGY & FUELS · OCTOBER 2009

Impact Factor: 2.79 · DOI: 10.1021/ef900458r

Energy Fuels **2009,** *23,* 4957–4965 · DOI:10.1021/ef900458r
Published on Web 08/28/2009

energy&fuels
article

Flame Propagation Speed of CO_2 Diluted Hydrogen-Enriched Natural Gas and Air Mixtures

Min Ji,[†] Haiyan Miao,*[,†,‡] Qi Jiao,[†] Qian Huang,[†] and Zuohua Huang[†]

[†]*State Key Laboratory of Multiphase Flow in Power Engineering, School of Energy and Power Eng., Xi'an Jiaotong University, China, and* [‡]*Institute of High Performance Computing, A-star, Singapore*

Received May 14, 2009. Revised Manuscript Received August 11, 2009

Adding hydrogen into natural gas can extend its lean burn capacity, improve engine performance at low load operation, and reduce unburned hydrocarbon emissions at the cost of increased NO_x emissions. In this paper, flame propagation of premixed CO_2 diluted natural gas/hydrogen/air mixtures under various initial pressures was studied by using a constant volume combustion bomb together with high-speed Schlieren photography. Laminar flame speed and laminar burning velocity as well as Markstein length and flame thickness were obtained for the diluted stoichiometric fuel/air mixtures with different natural gas/hydrogen fractions and diluent ratios under normal, reduced, and elevated pressures. The results showed that both unstretched flame speed and unstretched burning velocity are reduced with the increase of diluent ratio as well as initial pressure (except when the hydrogen fraction is 80%). Hydrogen-enriched natural gas with higher hydrogen fraction can tolerate relatively more diluent gas.

Introduction

With the growing crisis of petroleum resources and the environmental concern, clean alternative fuels have received more and more attention worldwide. Among many potential candidate fuels that can be used in passenger car engines, natural gas (mainly methane) is one of the most promising fuels and has already been used in many metropolises in the world. But due to its rather low value of burning velocity and high ignition energy requirement, the natural gas-fueled engines (either spark ignition type or pilot ignited dual fuel type) usually suffer from low efficiency and high unburned hydrocarbon at low load and idling operations and have poor lean burn capacity. The key to solving these problems lies in the improvement of the burning processes inside the combustion chamber. One method is to increase the burning velocity of natural gas by adding hydrogen into it. Experiments showed that using hydrogen-enriched natural gas can extend an engine's lean burn capacity, decrease cycle-to-cycle variation and therefore, reduce unburned hydrocarbon emission.[1−8]

However, adding hydrogen into natural gas enhances the formation of nitrogen oxide (NO_x); many engine tests evidenced that the more the hydrogen is added, the higher the NO_x emission is.[1,3,5] Exhaust gas recirculation (EGR) is one of the effective methods to reduce NO_x emission. Generally speaking, the introduction of exhaust gas into combustible mixtures decreases the combustion temperature as well as the oxygen concentration of the unburned gas, and both of these two effects reduce NO_x generation during the combustion process.[9] Knowledge on exhaust gas diluted combustion is required to effectively use EGR systems in an engine fueled with hydrogen-enriched natural gas.

Fundamental study on laminar combustion characteristics of a fuel provides basic information for both engine design and numerical model development. One of the most important properties of a fuel is its laminar burning velocity. It can not only represent laminar combustion characteristics, but also be used to simulate turbulent combustion (such as in ref 10) and provide basic knowledge for the investigation on the effect of flame stretch and wrinkling on premixed turbulent combustion,[11] which leads to improved understanding of the processes in spark ignition engines and power generation industry. Until now, the laminar burning characteristics of hydrogen enriched natural gas (or methane) have been studied intensively.[12−20]

*To whom correspondence should be addressed. Phone: 86-29-82665075 (Office). Fax: 86-29-82668789. E-mail: hymiao@mail.xjtu.edu.cn.

(1) Huang, Z.; Wang, J.; Liu, B.; Zeng, K.; Yu, J.; Jiang, D. *Energy Fuels* **2006**, *20* (2), 540–546.
(2) Huang, Z.; Liu, B.; Zeng, K.; Huang, Y.; Jiang, D.; Wang, X.; Miao, H. *Energy Fuels* **2007**, *21* (5), 2594–2599.
(3) Liu, B.; Huang, Z.; Zeng, K.; Chen, H.; Wang, X.; Miao, H.; Jiang, D. *Energy Fuels* **2008**, *22* (1), 273–277.
(4) Wang, J.; Chen, H.; Liu, B.; Huang, Z. *Int. J. Hydrogen Energy* **2008**, *33* (18), 4876–4883.
(5) Wang, J.; Huang, Z.; Fang, Y.; Liu, B.; Zeng, K.; Miao, H.; Jiang, D. *Int. J. Hydrogen Energy* **2007**, *32* (15), 3555–3564.
(6) Ma, F.; Wang, J.; Wang, Y.; Li, Y.; Liu, H.; Ding, S. *Energy Fuels* **2008**, *22* (3), 1880–1887.
(7) Ma, F.; Wang, Y. *Int. J. Hydrogen Energy* **2008**, *33* (4), 1416–1424.
(8) Ma, F.; Wang, Y.; Liu, H.; Li, Y.; Wang, J.; Ding, S. *Int. J. Hydrogen Energy* **2008**, *33* (2), 823–831.
(9) Heywood, J. B. *Internal Combustion Engine Fundamentals*; McGraw-Hill Book Company: New York, 1988; pp 103−105.
(10) Karpov, V.; Lipatnikov, A.; Zimont, V. Test of an engineering model of premixed turbulent combustion. *26th International Symposium on Combustion*;1996;pp 249−257.
(11) Jiang, D.; Chen, C.; Yang, J.; Yang, Z. *Advanced Internal Combustion Engine Fundamental*; Xi'an Jiaotong University Press:2006; pp 249−261.
(12) Yu, G.; Law, C.; Wu, C. *Combust. Flame* **1986**, *63* (1−2), 339–347.
(13) Karbasi, M.; Wierzba, I. *Int. J. Hydrogen Energy* **1998**, *23* (2), 123–129.
(14) Law, C.; Kwon, O. *Int. J. Hydrogen Energy* **2004**, *29* (8), 867–879.
(15) Halter, F.; Chauveau, C.; Djebayli-Chaumeix, N. *P. Combust. I.* **2005**, *30*, 201–208.
(16) Huang, Z.; Zhang, Y.; Zeng, K.; Liu, B.; Wang, Q.; Jiang, D. *Combust. Flame* **2006**, *146*, 302–311.
(17) Ilbas, M.; Crayford, A.; Yílmaz, İ.; Bowen, P.; Syred, N. *Int. J. Hydrogen Energy* **2006**, *31* (12), 1768–1779.
(18) Miao, H.; Jiao, Q.; Huang, Z.; Jiang, D. *Int. J. Hydrogen Energy* **2008**, *33*, 3876–3885.
(19) Lafay, Y.; Renou, B.; Cabot, G.; Boukhalfa, M. *Combust. Flame* **2008**, *153*, 540–561.
(20) Di Sarli, V.; Di Benedetto, A. *Int. J. Hydrogen Energy* **2007**, *32* (5), 637–646.

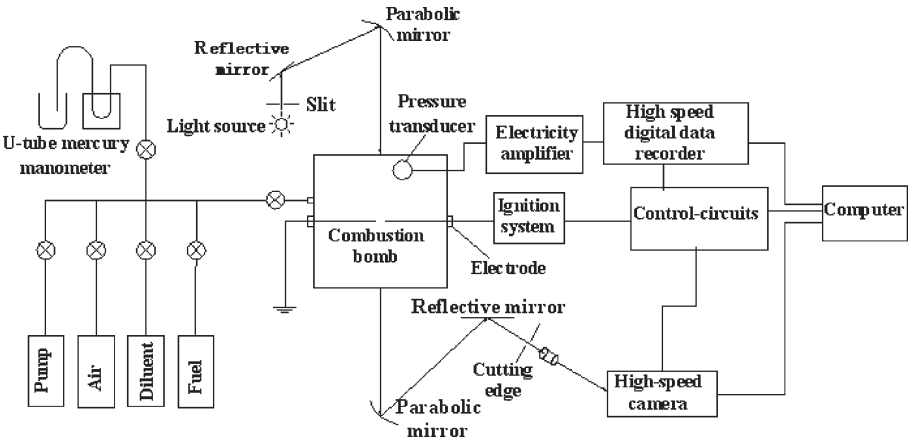

Figure 1. Experimental system arrangement.

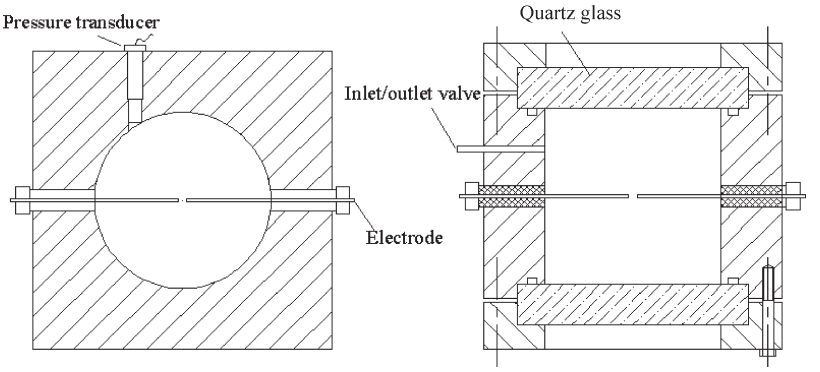

Figure 2. Structure of the constant volume combustion bomb.

To study the effect of exhaust gas, a mixture of nitrogen and carbon dioxide (CO_2) with a fixed ratio is usually used as diluents. For example, Han et al.[21] measured the burning velocity of methane/diluent/air mixture under various initial conditions. The diluent that was employed to simulate exhaust gas consisted of 18.5% CO_2 and 81.5% N_2. Elia et al.[22] used the mixture of 14% CO_2 and 86% N_2 to study the EGR effect on the burning velocity of methane, while Clarke et al.[23] employed the mixture of 15% CO_2 and 85% N_2 as diluent instead.

As we know, the main constituents of exhaust gas are nitrogen and CO_2, and their fractions in the exhaust gas vary with operation condition, type of the EGR system employed (cool or hot), and the fuel used. Therefore, it is rather difficult to choose a particular mixing ratio of nitrogen and CO_2, which can well represent real EGR from different combustion systems or even from the same engine but operating at different conditions. In our previous study, nitrogen and CO_2 were used as diluent gas respectively, and their effects on the combustion of diluted hydrogen enriched natural gas with different hydrogen fractions at various equivalence ratios were investigated separately.[24] Experimental results showed that CO_2 has stronger reduction effect on burning speed than nitrogen does. Recently, the laminar burning velocities of nitrogen-diluted hydrogen−natural gas and nitrogen diluted hydrogen−methane were reported.[25,26]

So far, there is lack of quantitative data on laminar combustion characteristics of carbon dioxide diluted hydrogen-enriched natural gas. This study aims at studying flame speed of carbon dioxide diluted hydrogen-enriched natural gas. In this paper, laminar flame speed, laminar burning velocity, Markstein length, and flame thickness of premixed stoichiometric CO_2 diluted natural gas−hydrogen−air mixtures with various diluent ratios under initial pressures of 0.08, 0.10, 0.15, and 0.20 MPa will be reported.

Experimental System and Procedure

Experiment System Arrangement. The experimental system used in this study includes a constant volume combustion bomb, ignition system, data acquisition system, and high-speed schlieren optical system as shown in Figure 1. A Redlake HG-100K high-speed CCD camera, operating at 10 000 pictures per second, was employed to record flame photographs. The constant volume combustion bomb (as illustrated in Figure 2) was a cylindrical type with a diameter and length of 130 mm. The two sides of the bomb were equipped with quartz glass windows to assess the optical results, thereby allowing observation of the combustion inside. A standard capacitive discharge ignition system with two electrodes located centrally was used to produce the spark and ignite the combustible mixture. In this study, the

(21) Han, P.; Checkel, M.; Fleck, B.; Nowicki, N. *Fuel* **2007**, *86*, 585–596.
(22) Elia, M.; Ulinski, M.; Metghalchi, M. *J. Eng. Gas Turbines Power-Trans. ASME* **2001**, *123* (1), 190–196.
(23) Clarke, A.; Stone, R.; Beckwith, P. *J. Inst. Energy* **1995**, *68* (476), 130–136.
(24) Miao, H.; Jiao, Q.; Huang, Z.; Jiang, D. *Int. J. Hydrogen Energy* **2009**, *34*, 507–518.
(25) Miao, H.; Ji, M.; Jiao, Q.; Huang, Q.; Huang, Z. *Int. J. Hydrogen Energy* **2009**, *34*, 3145–3155.
(26) Coppens, F.; Ruyck, J.; Konnov, A. *Combust. Flame* **2007**, *149*, 409–417.

Table 1. Constitution of Natural Gas

items	CH_4	C_2H_6	C_3H_8	N_2	CO_2	others
volumetric fraction (%)	96.160	1.096	0.136	0.001	2.540	0.067

ignition energy was 45 mJ. A piezoelectric Kistler pressure transducer was installed to measure the pressure inside the bomb.

Experiment Procedure. During the experiment, the combustible mixtures were prepared by introducing natural gas, hydrogen, air, and carbon dioxide according to their partial pressures, which were determined by initial pressure, natural gas fraction R_{NG} (the volume fraction of natural gas in hydrogen enriched natural gas), or hydrogen fraction R_{H_2} (the volume fraction of hydrogen in hydrogen enriched natural gas); equivalence ratio ϕ (the ratio of the actual fuel/air ratio to the stoichiometric ratio); and diluent ratio ϕ_r (the volume fraction of the diluent gas in the combustible mixture of natural gas, hydrogen, diluent gas, and air). As shown in Figure 2, the inlet/outlet valve was used to let fresh air in and combustion products out. Natural gas was admitted first, followed by hydrogen, then diluent gas and finally air. Enough time (at least 5 min) is required to obtain the quiescent mixture. The fuel−air mixture was then ignited by the centrally located electrodes. During the experiments, the initial pressure was set at 0.08, 0.1, 0.15, and 0.2 MPa, respectively, with constant initial temperature of 300 K.

In this study, hydrogen and CO_2 with purity of 99.995 and 99.99%, respectively, were used. The natural gas constitution is listed in Table 1, where the formula of natural gas is considered as $C_aH_bO_c$. Then, and shown in Table 1, it can be calculated that a, b, and c in $C_aH_bO_c$ are 1.015, 3.928, and 0.051, respectively.

Laminar Flame Speed and Laminar Burning Velocity

Intensive efforts have been undertaken to obtain the accurate value of the burning speed of a fuel. As a result, many techniques have been developed for this purpose, which generally can be classified into two categories depending on the usage of stationary flames (such as counterflow double flames [e.g., ref 12]) or nonstationary flames (such as outwardly propagating spherical flames [e.g., refs 27 and 28]). For a spherically expending flame, the stretch imposed on it is well-defined. Both asymptotic theories and experimental measurements have suggested that there exists a linear relationship between flame speed and flame stretch rate. Moreover, Markstein length (or Markstein number) can be derived while measuring the flame speed, which can be used to indicate flame stability. Therefore, the outwardly propagating spherical flame has been widely used to measure burning velocity. In this study, a constant volume combustion bomb was used to study the outwardly propagation spherical flames of CO_2 diluted hydrogen/natural gas/air mixtures.

For a spherically expanding flame, the stretched flame velocity (S_n), reflecting the flame propagation speed, is derived from the flame radius versus time data as

$$S_n = \frac{dr_u}{dt} \tag{1}$$

where r_u is the radius of flame in schlieren photographs, and t is the elapsed time from spark ignition. Note: to avoid the effects of spark and pressure rise, the flame radius was analyzed in the range of 6−25 mm, based on the observation of refs 29−31.

Flame stretch rate α in a quiescent mixture is defined as

$$\alpha = \frac{d(\ln A)}{dt} = \frac{1}{A}\frac{dA}{dt} \tag{2}$$

where A is the area of flame. For an outwardly propagating spherical flame without the occurrence of cellular structure, the flame stretch rate can be simplified as

$$\alpha = \frac{1}{A}\frac{dA}{dt} = \frac{2}{r_u}\frac{dr_u}{dt} = \frac{2}{r_u}S_n \tag{3}$$

During the early stage of flame expansion, there exists a linear relationship between the flame speeds and the flame stretch rates,[27] that is,

$$S_l - S_n = L_b\alpha \tag{4}$$

where L_b is the Markstein length of burned gases. Therefore, the unstretched flame speed (S_l) can be obtained as the intercept value at $\alpha = 0$ in the plot of S_n against α, and the burned gas Markstein length (L_b) is the slope of the $S_n-\alpha$ curve, which reflects the stability of the flame. A positive value of L_b indicates that the flame speed decreases with the increase of flame stretch rate. In this case, if any kinds of protuberances appear at flame front (stretch increasing), the flame speed at flame protruding position will be suppressed, and this makes the flame tend to be stable. On the contrary, a negative value of L_b means that the flame speed increases with the increase of flame stretch rate, that is, if any kinds of protuberances appear at flame front, the flame speed at flame protruding positions will be increased, and therefore the instability of flame increases.[28] When the observation is limited to the initial part of the flame expansion, where the pressure can be treated as a constant, there exists a simple relationship that links the spatial flame velocity (S_l) to unstretched laminar burning velocity (u_l) as shown below,

$$u_l = \rho_b S_l/\rho_u \tag{5}$$

where ρ_b and ρ_u are the densities for burned gases and unburned gases, respectively. The value of ρ_u was determined by ideal-gas equation of state, and that of ρ_b was determined from the calculated properties of the equilibrated adiabatic products.[31]

There exist two possible definitions for the stretched laminar burning velocity with the consideration of flame thickness (δ_l). As proposed by ref 28, the stretched laminar burning velocity at the unburned gas side is named as stretched laminar burning velocity (u_n), and that at the burned gas side as stretched mass burning velocity (u_{nr}), which are determined by eqs 6 and 7, respectively.

$$u_n = S\left[S_n\frac{\rho_b}{\rho_u}\right] \tag{6}$$

$$u_{nr} = \frac{\rho_b}{\rho_b - \rho_u}(u_n - S_n) \tag{7}$$

In eq 6, S is a rectified function that depends upon flame radius and density ratio and accounts for the effect of flame

(27) Gu, X.; Haq, M.; Lawes, M.; Woolly, R. *Combust. Flame* **2000**, *121* (1−2), 41–58.
(28) Bradley, D.; Gaskell, P.; Gu, X. *Combust. Flame* **1996**, *104* (1−2), 176–198.
(29) Lamoureux, N.; Djebaili-Chaumeix, N.; Paillard, C. *Exp. Therm. Fluid Sci.* **2003**, *27* (4), 385–393.
(30) Liao, S.; Jiang, D.; Cheng, Q. *Fuel* **2004**, *83* (9), 1247–1250.
(31) Bradley, D.; Hicks, R.; Lawes, M.; Sheppard, C.; Woolley, R. *Combust. Flame* **1998**, *115*, 126–144.

Table 2. Constitution of Test Fuels

tested fuels	fuel constitution	R_{NG} (%)	R_{H_2} (%)
fuel A	80 vol % natural gas + 20 vol % hydrogen	80	20
fuel B	60 vol % natural gas + 40 vol % hydrogen	60	40
fuel C	40 vol % natural gas + 60 vol % hydrogen	40	60
fuel D	20 vol % natural gas + 80 vol % hydrogen	20	80

Table 3. Test Conditions of Fuel A/Air/CO_2 Laminar Premixed Flame[a]

P_0 (MPa)	ϕ_r	S_l (m/s)	u_l (cm/s)	L_b	δ_l (mm)
0.08	0.0	3.22	41.5	1.26	0.05
0.08	0.05	2.14	27.0	1.89	0.08
0.08	0.1	1.37	17.1	2.33	0.11
0.08	0.15	0.82	10.2	2.95	0.18
0.1	0.0	2.88	37.0	0.77	0.04
0.1	0.05	1.90	24.0	1.45	0.07
0.1	0.1	1.20	15.0	1.68	0.10
0.1	0.15	0.70	8.7	1.91	0.17
0.15	0.0	2.53	32.4	0.33	0.03
0.15	0.05	1.65	20.8	0.49	0.05
0.15	0.1	1.04	13.0	0.82	0.08
0.15	0.15	0.61	7.6	1.43	0.13
0.2	0.0	2.15	27.4	0.18	0.03
0.2	0.05	1.40	17.6	0.25	0.04
0.2	0.1	0.88	10.9	0.51	0.06
0.2	0.15	0.53	6.5	0.73	0.10

[a] Fuel A, R_{NG} = 80%, R_{H_2} = 20%, ϕ = 1.0, T_0 = 300 K.

Table 4. Test Conditions of Fuel B/Air/CO_2 Laminar Premixed Flame[a]

P_0 (MPa)	ϕ_r	S_l (m/s)	u_l (cm/s)	L_b	δ_l (mm)
0.08	0.0	3.99	51.7	0.53	0.05
0.08	0.05	2.50	31.8	1.08	0.07
0.08	0.1	1.70	21.4	1.86	0.10
0.08	0.15	1.10	13.8	2.25	0.16
0.1	0.0	3.48	45.1	0.34	0.04
0.1	0.05	2.16	27.5	0.67	0.07
0.1	0.1	1.46	18.3	1.06	0.10
0.1	0.15	0.93	11.6	1.45	0.15
0.1	0.2	0.58	7.4	2.19	0.22
0.15	0.0	3.24	41.8	0.19	0.03
0.15	0.05	2.05	25.9	0.29	0.05
0.15	0.1	1.34	16.7	0.57	0.07
0.15	0.15	0.82	10.3	1.10	0.11
0.15	0.2	0.48	6.0	1.48	0.18
0.2	0.0	2.81	36.1	0.11	0.02
0.2	0.05	1.78	22.5	0.24	0.03
0.2	0.1	1.15	14.4	0.32	0.05
0.2	0.15	0.70	8.7	0.53	0.08

[a] Fuel B, R_{NG} = 60%, R_{H_2} = 40%, ϕ = 1.0, T_0 = 300 K.

thickness on the mean density of the burned gases. The expression of S used in the present study was given in ref 28 as below.

$$S = 1+1.2\left[\frac{\delta_l}{r_u}\left(\frac{\rho_u}{\rho_b}\right)^{2.2}\right]-0.15\left[\frac{\delta_l}{r_u}\left(\frac{\rho_u}{\rho_b}\right)^{2.2}\right]^2 \quad (8)$$

Results and Discussion

In this section, the laminar flame speed and the laminar burning velocity of stoichiometric CO_2 diluted hydrogen/natural gas/air mixtures with various natural gas fractions (20, 40, 60, and 80%) and diluent ratios (from 0 to 0.20 at the interval of 0.05) under different initial pressures will be provided. The effects of fuel constitution, diluent ratio, and initial pressure on flame propagation speed will be discussed.

Table 5. Test Conditions of Fuel C/Air/CO_2 Laminar Premixed Flame[a]

P_0 (MPa)	ϕ_r	S_l (m/s)	u_l (cm/s)	L_b	δ_l (mm)
0.08	0.0	4.94	64.8	0.42	0.05
0.08	0.05	3.32	42.8	0.71	0.06
0.08	0.1	2.22	28.3	0.97	0.09
0.08	0.15	1.47	18.6	1.48	0.14
0.08	0.2	0.80	10.2	2.27	0.24
0.1	0.0	4.72	61.9	0.24	0.03
0.1	0.05	3.16	40.7	0.40	0.05
0.1	0.1	2.06	26.3	0.58	0.08
0.1	0.15	1.34	16.9	0.87	0.12
0.1	0.2	0.74	9.3	1.43	0.21
0.15	0.0	4.18	54.6	0.10	0.03
0.15	0.05	2.80	35.8	0.22	0.04
0.15	0.1	1.78	22.5	0.34	0.06
0.15	0.15	1.20	15.1	0.65	0.09
0.15	0.2	0.67	8.5	0.95	0.15
0.2	0.0	3.80	49.5	0.00	0.02
0.2	0.05	2.51	32.1	0.12	0.02
0.2	0.1	1.64	20.7	0.26	0.03
0.2	0.15	1.126	14.2	0.36	0.05

[a] Fuel C, R_{NG} = 40%, R_{H_2} = 60%, ϕ = 1.0, T_0 = 300 K.

Table 6. Test Conditions of Fuel D/Air/CO_2 Laminar Premixed Flame[a]

P_0 (MPa)	ϕ_r	S_l (m/s)	u_l (cm/s)	L_b	δ_l (mm)
0.08	0.0	6.67	89.5	0.31	0.04
0.08	0.05	4.61	60.7	0.54	0.06
0.08	0.1	2.83	36.9	0.64	0.09
0.08	0.15	1.98	25.7	0.71	0.12
0.08	0.2	1.07	13.9	0.78	0.22
0.1	0.0	7.37	98.7	0.24	0.03
0.1	0.05	5.24	68.9	0.36	0.04
0.1	0.15	2.15	27.7	0.47	0.09
0.1	0.2	1.20	15.6	0.70	0.16
0.15	0.0	7.62	101.7	0.09	0.02
0.15	0.05	5.27	69.1	0.17	0.03
0.15	0.1	3.26	42.1	0.19	0.04
0.15	0.15	2.24	28.8	0.21	0.06
0.15	0.2	1.37	17.6	0.26	0.09
0.2	0.0	6.26	83.3	−0.07	0.09
0.2	0.05	4.36	56.9	0.09	0.01
0.2	0.1	2.66	34.3	0.12	0.02
0.2	0.15	1.77	22.8	0.19	0.03
0.2	0.2	0.93	11.9	0.20	0.06

[a] Fuel D, R_{NG} = 20%, R_{H_2} = 80%, ϕ = 1.0, T_0 = 300 K.

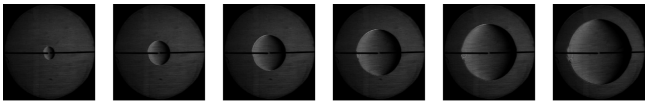

Figure 3. Schlieren images captured by high-speed camera during flame development. (Fuel C, P_0 = 0.10 MPa, ϕ = 1.0, ϕ_r = 0.1).

To represent hydrogen-enriched natural gas with different amount of hydrogen addition, four test fuels named fuel A, fuel B, fuel C, and fuel D were used in this study. The constitution of these four test fuels are listed in Table 2. The test conditions are summarized in Tables 3−6.

Schlieren photographs (as shown in Figure 3) taken during the experiment were measured to obtain the flame radius at different time after ignition. Figure 4 illustrates some of the measured results of the flame radius versus the time after ignition. Fuels A and D were chosen to represent

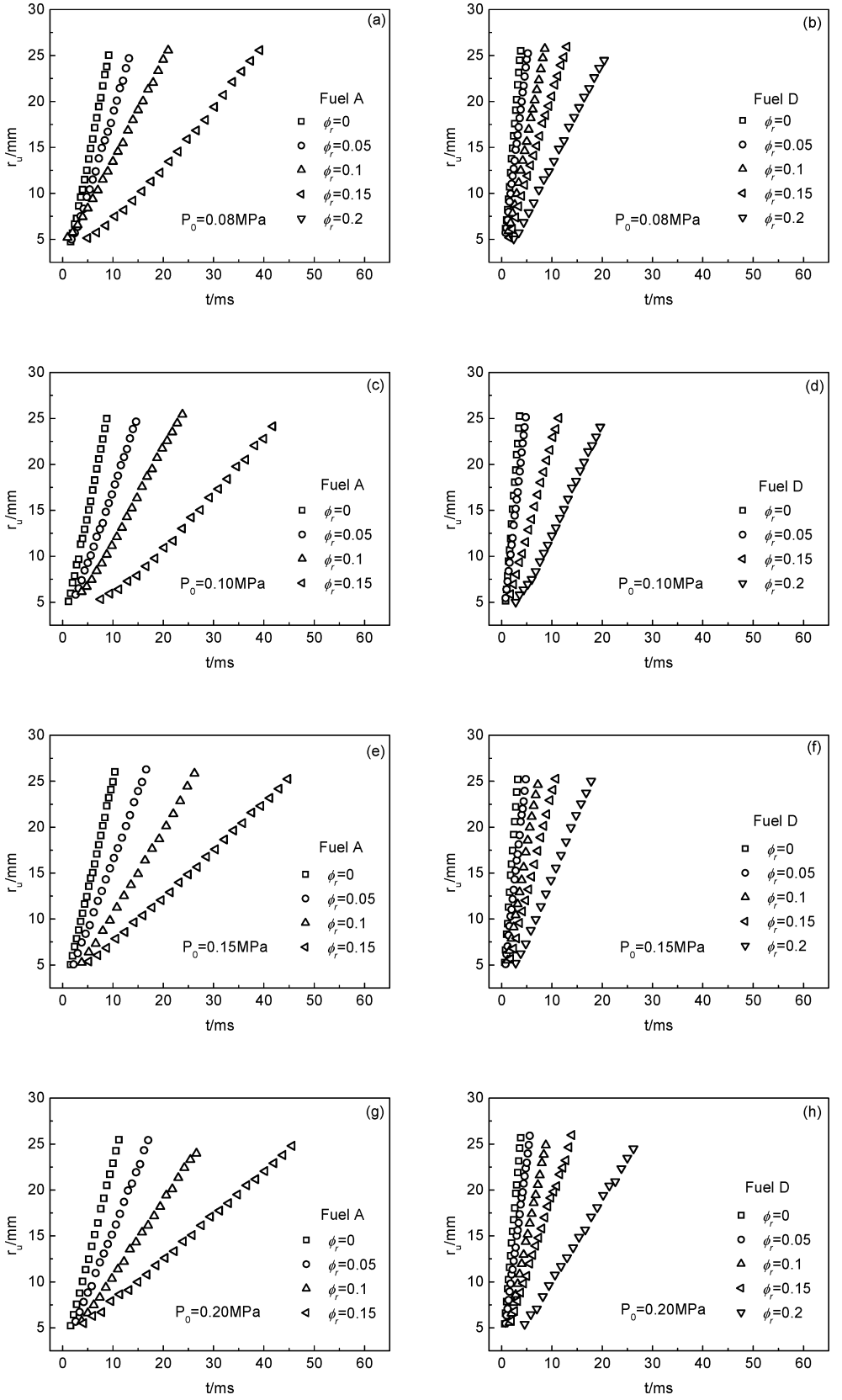

Figure 4. Flame development of CO_2 diluted hydrogen enriched natural gas at various diluent ratios and initial pressures. (ϕ = 1.0).

hydrogen-lean and hydrogen-rich fuels, respectively. By comparing Figure 4a with 4b, Figure 4c with 4d, Figure 4e with 4f, and Figure 4g with 4h, the effect of hydrogen addition and diluent ratio on the flame velocity can be observed. It clearly shows that, with the increase of hydrogen fraction from 20 to 80% (or the decrease of natural gas fraction from 80 to 20%), the flame expands much faster. On the other hand, adding CO_2 slows down the process of flame propagation. The more the CO_2 is added, the more the flame speed is reduced. Figure 4 also suggested that the reduction effect of the diluent gas is

determined not only by the diluent ratio, but also by the constitution of the fuel.

The goal of this study is to investigate the effect of diluent ratio on the laminar combustion characteristics of CO_2 diluted hydrogen-enriched natural gas/air mixtures under different initial pressures. Experiments were conducted under reduced (0.08 MPa), ambient or normal (0.1 MPa), and elevated (0.15 and 0.2 MPa) pressures, respectively. Results showed that with the increase of the initial pressure, the flame propagation tends to be retarded in most cases. For Fuels A, B, and C, the increase of the initial pressure slows down the process of flame propagation monotonically (using the case of Fuel A as a representative, see Figures 4a, 4c, 4e and 4g). However, when the hydrogen fraction reaches 80% (Fuel D), the effect of the initial pressure showed a more complex pattern. By comparing Figures 4b, 4d, 4f, and 4h, it can be seen that with the increase of the initial pressure, the flame propagates at a faster speed at first (the pressure rises from 0.08 to 0.15 MPa), and then stars to slow down with the further increase of the initial pressure (from 0.15 to 0.2 MPa).

Furthermore, the effect of the initial pressure relates not only to the fuel constitution, but also to the amount of the diluent gas. Figure 4 also suggested that these highly diluted mixtures tend to be much more sensitive to the change of the initial pressure. Our previous results showed that the flame speed is reduced with the increase of the CO_2 diluent ratio under ambient pressure due to both thermal and chemical effects.[24] The experimental results of this study will allow us to obtain a better understanding on the reduction effect of the diluent gas under both reduced and elevated initial pressures.

As mentioned in the previous section, the stretched flame speed is defined as a derivative of flame radius with time, which reflects the flame propagating speed relative to the combustion wall. To obtain unstretched flame speed, the stretched flame speed versus the flame stretch rate need to be plotted. Using the experimental results of Fuel C as an example, Figure 5 illustrates how to obtain the value of unstretched flame speed from a $S_n-\alpha$ plot. As shown in Figure 5, the unstretched flame speed S_l can be obtained by extending the experimental results to zero flame stretch rate. By repeating the analysis process to all the experimental data, we then obtained the unstretched flame speeds of stoichiometric fuel/air mixtures under different initial pressures.

The unstretched flame speeds obtained in this study are summarized in Figure 6. The effect of initial pressure on flame propagation is clearly illustrated. Figures 6a, 6b, and 6c show that for Fuels A, B, and C, with the increase of the initial pressure the flame speed is reduced monotonically. On the

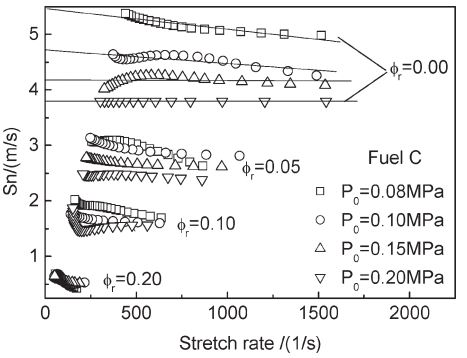

Figure 5. Stretched flame speed versus stretch rate at various initial pressures and diluent ratios (ϕ = 1.0).

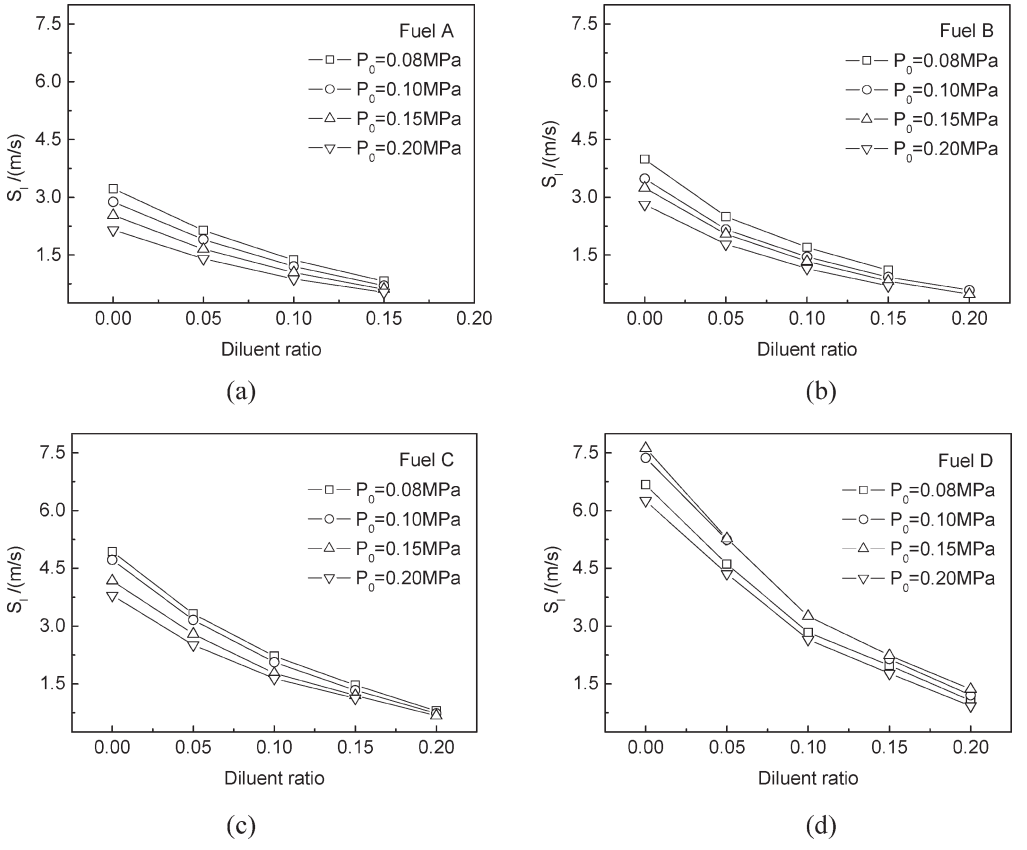

Figure 6. Unstretched flame speed versus diluent ratio at various initial pressures (ϕ = 1.0).

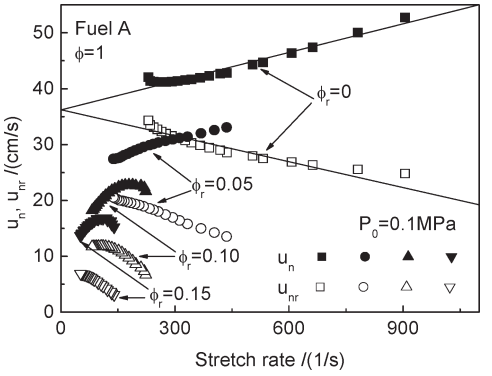

(a)

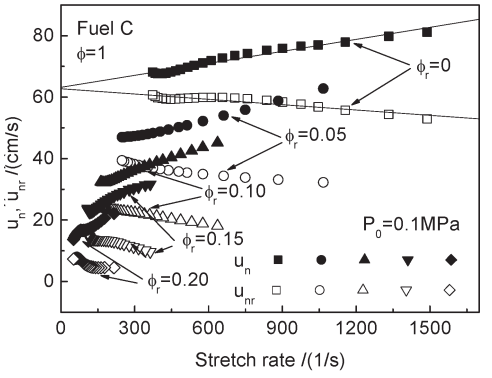

(b)

Figure 7. Effect of diluent ratio on stretched burning velocity.

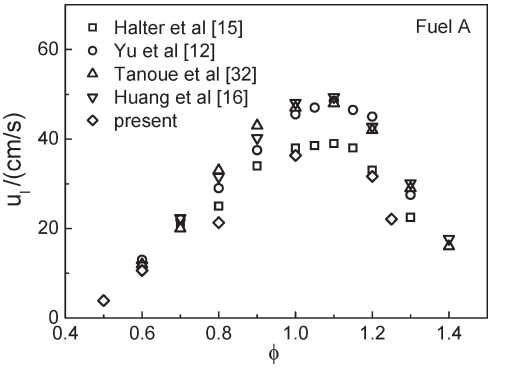

Figure 8. Unstretched laminar burning velocity of fuel A/air mixture versus equivalence ratio (P_0 = 0.1 MPa).

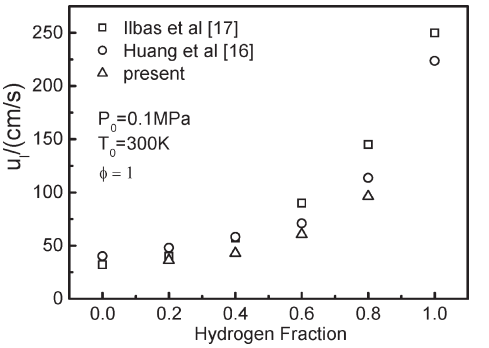

Figure 9. Unstretched laminar burning velocity of NG/hydrogen/air mixture versus hydrogen fraction.

other hand, in the case of Fuel D, the flame speed increases with the increase of the initial pressure from 0.08 to 0.15 MPa at first, and then starts to decrease with the further increase of the initial pressure from 0.15 to 0.2 MPa (see Figure 6d). The enhancement effect of the hydrogen addition and the retardation effect of the diluent gas on the flame propagation can also be observed in Figure 6.

Figure 7 illustrates the difference between the stretched laminar burning velocity u_n and the stretched mass burning velocity u_{nr} for the fuel/air mixtures with different diluent ratios. The stretched laminar burning velocity, which indicates the rate of the mixture entrainment, increases with the increase of the stretch rate. On the other hand, the stretched mass burning velocity, whose definition is related to the production of burned gas, usually decreases with the increase of the stretch rate. Consequently, the difference between u_n and u_{nr}, that is, $u_n - u_{nr}$, increases with the increase of the stretch rate. As a result, the value of $u_n - u_{nr}$ is relatively large at high stretch rate where flame radius is small and the effect of the flame thickness can not be ignored. At zero stretch rate (i.e., the flame radius becomes infinity), the effect of the flame thickness then becomes negligible, therefore u_n and u_{nr} will reach at the same value, that is, the unstretched laminar burning velocity (u_l). As shown in Figure 7, the difference between u_n and u_{nr} is enlarged with the increase of the diluent ratio.

Before discussing the effect of diluent ratio and initial pressure on unstretched burning velocity, we compared our results with the data reported in literatures (mainly obtained under normal pressure and temperature). As shown in Figures 8 and 9, the agreement is reasonably well. Note: in refs 12, 15, and 32, the test fuel was 20% hydrogen and 80% methane; in ref 17, the test fuel was hydrogen-enriched methane.

The measured unstretched burning velocities of stoichiometric CO_2 diluted hydrogen-enriched natural gas/air mixtures with various diluent ratios under different initial pressures are summarized in Figure 10. By comparing Figure 10 with Figure 6, it can be seen that the effects of initial pressure, diluent ratio, and hydrogen fraction on the unstretched burning velocity are similar to these on the unstretched flame speed. It appears that hydrogen-enriched natural gas with higher hydrogen fraction can tolerate a relatively larger amount of diluent gas. From Figure 10, it was observed that the effect of the initial pressure on the burning velocity of CO_2 diluted fuel/air mixtures is the same as the corresponding nondiluted one.

Figure 10 shows that the effect of initial pressure is affected by fuel constitution. For the fuel with hydrogen fraction less than and equal to 60% (fuels A, B, and C), with the increase of initial pressure the burning velocity reduces monotonically (see Figure 10a, 10b, and 10c). This agrees well with the study results which indicated that the burning velocity of methane and natural gas reduces gradually with the increase of the initial pressure.[27,33,34] For the fuel with hydrogen fraction of 80% (fuel D), the burning velocity increases with the increase of the initial pressure from 0.08 to 0.15 MPa at first, and then starts to decreases with the further increase of the initial pressure from 0.15 to 0.2 MPa (See Figure 10d).

(32) Tanoue, K.; Goto, S.; Shimada, F.; Hamatake, T. *Trans. Jap. Soc. Mech. Eng., Part B* **2003**, *69*, 162–168.

(33) Andrews, G.; Bradley, D. *Combust. Flame* **1972**, *19*, 275–288.

(34) Stone, R.; Clarke, A.; Beckwith, P. *Combust. Flame* **1998**, *114*, 546–555.

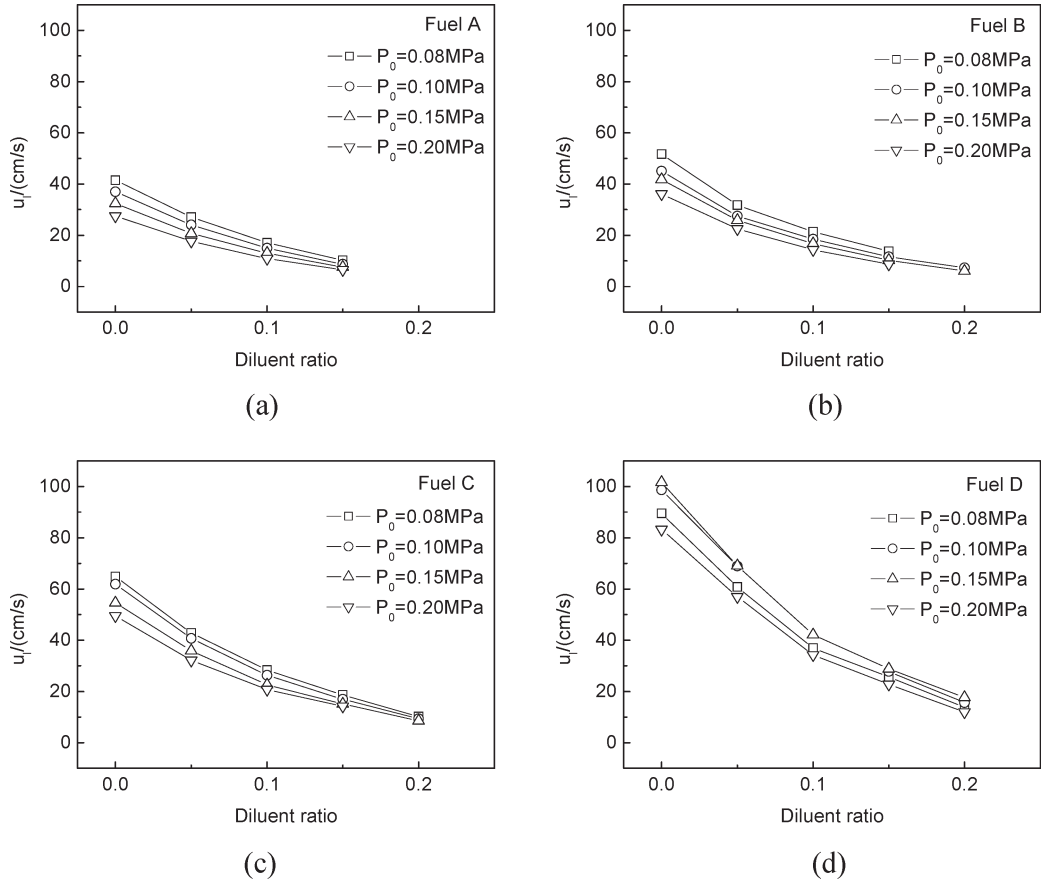

Figure 10. Unstretched burning velocity versus diluent ratio at various initial pressures (ϕ = 1.0).

Generally speaking, initial pressure has two effects on the flame: chemical effect (related to radical concentration) and thermal effect (in term of flame temperature).[11] It was found that radical (such as H and OH) concentration decreases with elevated pressure[35] and the flame speed tends to decline with the increase of initial pressure. On the other hand, the increment of initial pressure will increase the temperature of the reaction zone, which can prompt the reaction rate. Therefore, it depends on the balance of these two effects to determine whether the increment of initial pressure is favorable or unfavorable to the flame propagation. As illustrated by Figure 10, hydrogen-enriched natural gas obeys the similar rule as methane or natural gas does until the fuel is highly enriched by hydrogen (fuel D). This indicates that in most cases the chemical effect is the dominant factor, and with the increase of the initial pressure, the benefit obtained from the increased flame temperature cannot balance the negative effect of the reduction of radical concentration on the flame propagation. Only for the fuel with very high hydrogen fraction (80% in this study) does the thermal effect overtake the reduction effect of radical concentration when the initial pressure increased from 0.08 to 0.15 MPa. The further increase of the initial pressure sees that the chemical effect dominates again.

Conclusions

Experiments were conducted to study the effect of diluent gas on flame propagation speed of hydrogen-enriched natural gas under different initial pressures in a constant volume combustion bomb. Unstretched flame speed and unstretched burning velocity of stoichiometric CO_2 diluted hydrogen/natural gas/air mixtures with various hydrogen fractions and diluent ratios under normal, reduced, and elevated initial pressures were obtained. It was found that both unstretched flame speed and unstretched burning velocity are reduced with the increase of diluent ratio as well as initial pressure (except when the hydrogen fraction is 80%), and increased with the increase of hydrogen fraction. The effect of initial pressure on the flame speed of diluted hydrogen-enriched natural gas/air mixtures obeys the same rule as that of the corresponding nondiluted ones.

Nomenclature

a = Number of C atoms for a general fuel of average molecular composition $C_aH_bO_c$
A = Flame area (m^2)
b = Number of H atom for a general fuel of average molecular composition $C_aH_bO_c$
c = Number of O atom for a general fuel of average molecular composition $C_aH_bO_c$
f = Mass burning flux ($g\ cm^{-1}s^{-1}$)
L_b = Markstein length of burned gases
P_0 = Initial pressure (MPa)
r_u = Flame radius (mm)
R_{NG} = Natural gas volumetric fraction of hydrogen enriched natural gas
R_{H_2} = Hydrogen volumetric fraction of hydrogen enriched natural gas
S_l = Unstretched flame speed (m/s)
S_n = Stretched flame speed (m/s)

(35) Westbrook, C.; Dryer, F. *Combust. Flame* **1980**, *37*, 171–192.

t = Time (s)
u_l = Unstretched laminar burning velocity (m/s)
u_n = Stretched laminar burning velocity (m/s)
u_{nr} = Stretched mass burning velocity (m/s)
ρ_b = Density of burned gases (kg/m^3)
ρ_u = Density of unburned gases (kg/m^3)
α = Flame stretch rate (s^{-1})
ϕ = Equivalence ratio
ϕ_r = Diluent ratio
δ_l = Flame thickness (mm)
ν = Kinematic viscosity of unburned gas (m^2/s)

Acknowledgment. This work is supported by the National Natural Science Foundation of China (No. 50606029), the National Basic Research Program (No. 2007CB210006) and the Scientific Research Foundation for ROCS, State Education Ministry.